Letter

Optimizing the random search of a finite-lived target by a Lévy flight

Denis Boyer,[1,*] Gabriel Mercado-Vásquez,[2,†] Satya N. Majumdar,[3,‡] and Grégory Schehr[4,§]

[1]*Instituto de Física, Universidad Nacional Autónoma de México, Ciudad de México 04510, México*
[2]*Pritzker School of Molecular Engineering, University of Chicago, Chicago, Illinois, 60637, USA*
[3]*LPTMS, CNRS, Univ. Paris-Sud, Université Paris-Saclay, 91405 Orsay, France*
[4]*Sorbonne Université, Laboratoire de Physique Théorique et Hautes Energies, CNRS UMR 7589, 4 Place Jussieu, 75252 Paris Cedex 05, France*

(Received 11 October 2023; accepted 22 January 2024; published 14 February 2024)

In many random search processes of interest in chemistry, biology, or during rescue operations, an entity must find a specific target site before the latter becomes inactive, no longer available for reaction or lost. We present exact results on a minimal model system, a one-dimensional searcher performing a discrete time random walk, or Lévy flight. In contrast with the case of a permanent target, the capture probability and the conditional mean first passage time can be optimized. The optimal Lévy index takes a nontrivial value, even in the long lifetime limit, and exhibits an abrupt transition as the initial distance to the target is varied. Depending on the target lifetime, this transition is discontinuous or continuous, separated by a nonconventional tricritical point. These results pave the way to the optimization of search processes under time constraints.

DOI: 10.1103/PhysRevE.109.L022103

Random search processes are ubiquitous in nature, such as animals searching for food [1,2], rescue operations looking for survivors after a shipwreck [3,4], or even searches for a lost object like a key or a wallet. In typical search models, one considers the targets to be "immortal", i.e., they do not disappear after a certain time. During the last decades, several models of random search of infinitely lived targets have been studied. The most popular among them is the search by a random walker, either diffusive or performing Lévy flights where the jumps are long ranged. Several strategies have been incorporated to make the search by a random walker optimal. Lévy walks with certain exponent values can maximize the capture rate by a forager of dispersed resources [5–12]. Another well known strategy is the intermittent search process where short range and long range moves alternate to locate a single target [13,14]. A popular model that has received much attention in recent years is a resetting random walker, where the walker goes back to its starting point with a finite probability after every step and restarts the search process [15–23]. In this case, it turns out that the mean time to find an infinitely lived target can be minimized by choosing an optimal resetting probability [15,16,22,24–33]. This fact has also been verified in recent experiments in optical traps [34–36].

However, there are many instances where the target has a finite but random lifetime. For instance, ripe fruits in a tree rot in a few days. The lifetime of a fruit is typically random since it depends on the nature of the tree and the weather [37]. Similarly, after a shipwreck, a survivor can last in the water only a finite amount of time, which is random as it depends on the general health of the person and sea conditions [38]. Inside a cell, target sites along the DNA are often blocked for long periods of time, which gives a limited random time to the transcription factors to bind to them [39–41]. In many examples, the searcher has to capture the target before it disappears or dies. Alternatively, in a dual view, one can consider the target as permanent and the walker with a strong time constraint, as an aerial rescue vehicle having a limited flight time [42]. The termination of the search at a random time also appears in the context of foraging theory, where a searcher abandons a patch at any time with a certain give up probability [43]. For a mortal searcher performing a lattice random walk [44] or Brownian motion [45], the capture probability and conditional mean first-passage time cannot be optimized, or only with an infinite diffusion coefficient. If a resetting mechanism is further implemented, though, a nonzero resetting rate can be optimal provided the mortality rate is not too high [46,47].

A general question then is: is there any way to optimize the search success for a nonpermanent target with a random lifetime? A natural generalization of the Brownian case is to investigate the search by a Lévy flight with a Lévy exponent $0 < \mu < 2$. One can then ask whether there is an optimal value of μ that minimizes the conditional search time or, alternatively, maximizes the capture probability of the mortal target. In this Letter, we address this problem for a one-dimensional Lévy flight (see Fig. 1). In our model, the target is fixed at the origin and its lifetime n is distributed geometrically via $p(n) = (1 - a)\, a^n$ where $0 < a < 1$, i.e., at each discrete step, the target dies with probability $1 - a$ and keeps alive with the complementary probability a. We assume that the Lévy searcher starts from $x_0 > 0$ and subsequently evolves in discrete time via

$$x_n = x_{n-1} + \eta_n, \tag{1}$$

*boyer@fisica.unam.mx
†gabrielmv.fisica@gmail.com
‡satya.majumdar@universite-paris-saclay.fr
§gregory.schehr@u-psud.fr

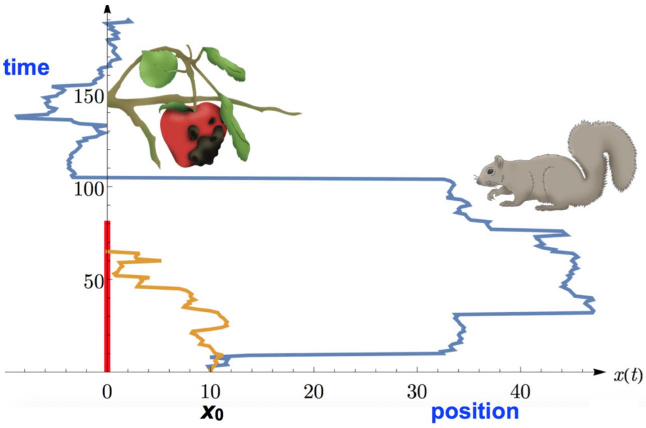

FIG. 1. A searcher, performing a Lévy flight in one-dimension, is looking for a nonpermanent target (i.e., a ripe fruit) located at the origin. At each time step, the target (in red) stays active with probability $a < 1$, while the searcher performs a random step. If the searcher finds the target in the active state, the search is successful (orange trajectory). In contrast, if the target dies (rots) before being found by the searcher, the search is unsuccessful (blue trajectory).

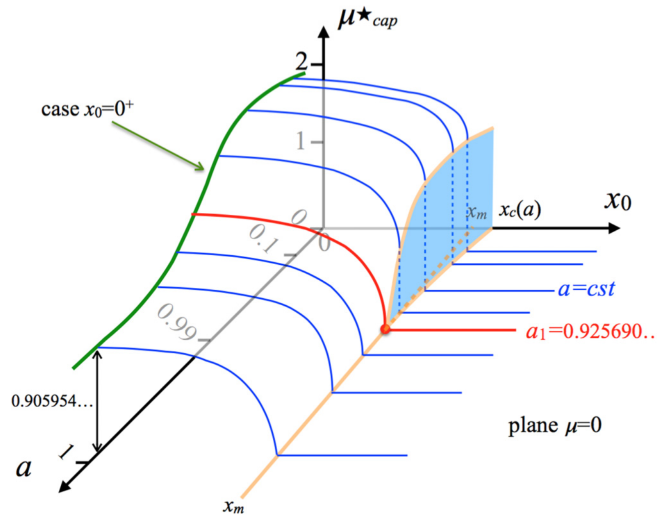

FIG. 2. Schematic phase diagram of the optimal Lévy index $\mu^*_{\rm cap}$ in the (x_0, a) plane. For fixed a, as a function of x_0, the optimal $\mu^*_{\rm cap}$ undergoes a first-order transition at $x_0 = x_c(a)$ (for $a < a_1$) which changes to a second-order transition for $a > a_1$. The critical line $x_c(a)$ freezes to $x_m = 0.561459\ldots$ for $a > a_1$. The point that separates the first-order and second-order transitions is a tricritical point (shown by the red dot).

where η_n's are independent and identically distributed jump variables, each distributed via the probability distribution function $f(\eta)$, which we assume to be symmetric and continuous with a power-law tail $\propto 1/|\eta|^{1+\mu}$ where $\mu \in (0, 2)$. Note that both parameters x_0 and a are given numbers and the searcher has no control in optimizing with respect to them. Thus, the only parameter that the searcher has in her disposal to optimize is μ, since it is associated with her motion. The search is successful only if the walker crosses the origin for the first time (takes $x_n < 0$) while the target is still alive. We characterize the search success by two different observables: (i) the capture probability of the target and (ii) the conditional mean first-passage time (CMFPT), i.e., the mean search time conditioned to finding the target alive. We find that, for fixed x_0 and a, these two quantities can be optimized by varying the Lévy index μ. The two optimal parameters $\mu^\star_{\rm cap}(x_0, a)$ and $\mu^\star_{FP}(x_0, a)$ exhibit very rich phase diagrams in the (x_0, a) plane.

Our results, obtained analytically and numerically, are summarized schematically in Fig. 2 for the capture probability. For any fixed $a < a_1 = 2\,e\,(\sqrt{15} - 2)/11 = 0.925690\ldots$, the index $\mu^\star_{\rm cap}(x_0, a)$ decreases monotonically as a function of x_0, and jumps to zero abruptly at a critical value $x_0 = x_c(a)$. This signals a first-order transition. In contrast, for any $a > a_1$, $\mu^\star_{\rm cap}(x_0, a)$ again decreases with x_0 but vanishes continuously at $x_c(a)$, signaling a second-order transition. In the case $a > a_1$, the critical value $x_c(a)$ freezes to a constant value $x_c(a) = x_m$. Thus, (x_m, a_1), shown by a red dot in Fig. 2, is a tricritical point that sits at the junction of a first and second-order transition. The green line $x_0 \to 0$ is obtained analytically in the Supplemental Material [48]. A qualitatively similar diagram can be drawn for $\mu^\star_{FP}(x_0, a)$, with a tricritical point at a slightly larger value $a_2 = 0.973989\ldots$ [48].

Both observables, the capture probability and the CMFPT, can be related to one fundamental quantity $Q_\mu(x_0, n)$ associated with the random walk, denoting the probability that a Lévy flight with index μ, starting at $x_0 \geqslant 0$, does not cross zero up to step n [17,49,52–59]. Consequently, $Q_\mu(x_0, n-1) - Q_\mu(x_0, n)$ is the probability that the Lévy flight crosses the origin for the first time at the nth step, with $Q_\mu(x_0, n = 0) = 1$. Thus, for the target to be captured at the nth step, it has to remain alive at least up to step $n-1$, which occurs with probability a^{n-1}. Therefore, the capture probability $C_\mu(x_0, a)$, defined as the probability that the searcher starting at x_0 finds the target before the latter becomes inactive, is given by $C_\mu(x_0, a) = \sum_{n=1}^{\infty} a^{n-1}[Q_\mu(x_0, n-1) - Q_\mu(x_0, n)]$. This sum can be rewritten as

$$C_\mu(x_0, a) = \frac{1 - (1-a)\widetilde{Q}_\mu(x_0, s = a)}{a}, \qquad (2)$$

where $\widetilde{Q}_\mu(x_0, s) \equiv \sum_{n=0}^{\infty} s^n Q_\mu(x_0, n)$ is the generating function of $Q_\mu(x_0, n)$. Similarly, the CMFPT $T_\mu(x_0, a)$, the mean time taken by the successful trajectories to locate the target [45], can be expressed as $T_\mu(x_0, a) = \sum_{n=1}^{\infty} n a^{n-1}[Q_\mu(x_0, n-1) - Q_\mu(x_0, n)]/C_\mu(x_0, a)$, where $C_\mu(x_0, a)$ acts as a normalization factor. This can also be rewritten again in terms of the generating function of the survival probability

$$T_\mu(x_0, a) = a\frac{\partial}{\partial a}\ln[1 - (1-a)\widetilde{Q}_\mu(x_0, s = a)]. \qquad (3)$$

Thus, to analyze either $C_\mu(x_0, a)$ or $T_\mu(x_0, a)$, we need the generating function $\widetilde{Q}_\mu(x_0, s)$ for Lévy flights. Unfortunately, there is no simple expression for $\widetilde{Q}_\mu(x_0, s)$. However, its Laplace transform with respect to x_0 is given by the exact Pollaczek-Spitzer formula [52,53],

$$\int_0^\infty \widetilde{Q}_\mu(x_0, s)\, e^{-\lambda x_0} dx_0 = \frac{1}{\lambda\sqrt{1-s}}\varphi(\lambda, s) \qquad (4)$$

$$\text{with} \quad \varphi(\lambda, s) = \exp\left[-\frac{\lambda}{\pi}\int_0^\infty \frac{\ln[1 - s\hat{f}(k)]}{\lambda^2 + k^2}dk\right], \qquad (5)$$

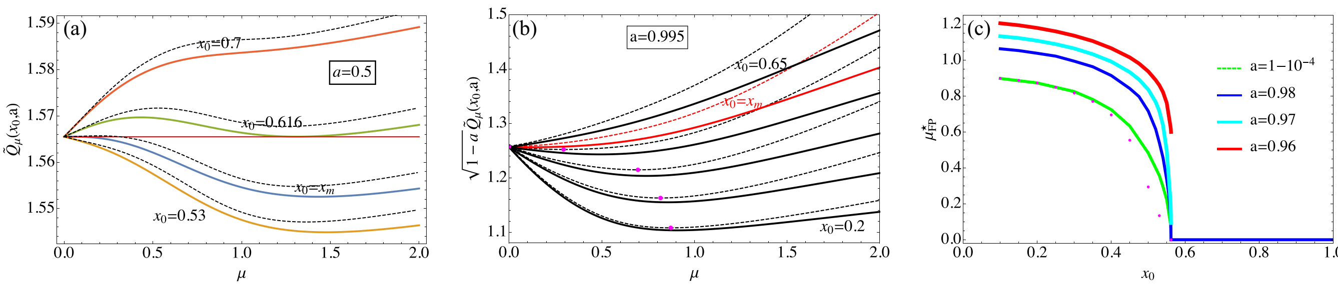

FIG. 3. (a) Discontinuous transition with short-lived targets ($a = 0.5$): numerical $\widetilde{Q}_\mu(x_0, a)$ vs μ for different starting positions close to x_m. (b) Continuous transition for long-lived targets (a close to 1): $\sqrt{1-a}\widetilde{Q}_\mu(x_0, a)$ as a function of μ and for several x_0 around x_m. In (a) and (b) the dotted lines represent the concavity approximation (12). (c) Optimal exponent for the CMFPT as a function of x_0 for various a. Below $a_2 = 0.973989...$, the transition is discontinuous ($a = 0.97$), while it is continuous above ($a = 0.98$). The dots correspond to the minima in (b), given by the concavity approximation. The index $\mu^\star_{\text{cap}}(x_0, a)$ has analogous variations near a_1.

where $\hat{f}(k) = \int_{-\infty}^{\infty} f(\eta)\, e^{ik\eta} d\eta$ is the Fourier transform of the step distribution. Here we will focus on Lévy stable jump distribution, with $\hat{f}(k) = e^{-|k|^\mu}$ with $0 < \mu \leqslant 2$.

With an infinite-lived target ($a = 1$), recall that $C_\mu = 1$, owing to the recurrence property of $1d$ random walks, while $T_\mu = \infty$, independently of x_0 and $f(\eta)$ [60]. Hence, there is no option of optimizing them by varying μ. However, for a finite-lived target where $a < 1$, both quantities become nontrivial functions of μ and can be optimized by choosing μ appropriately with optimal values $\mu^\star_{\text{cap}}(x_0, a)$ and $\mu^\star_{FP}(x_0, a)$. One finds that, even for short-lived targets, C_μ at optimality can be larger than the maximal value $1/2$ that could be achieved by a naive ballistic strategy (see [48]).

In order to maximize the capture probability in Eq. (2) by varying μ, for fixed x_0 and a, it turns out that we need to minimize $\widetilde{Q}_\mu(x_0, s = a)$ with respect to μ. We will study the exact relation in Eq. (4), both analytically in certain limits and numerically by inverting the Laplace transform in Eq. (4) using the Gaver-Stehfest method [50,51], which we explain in [48].

We start by plotting the numerically obtained $\widetilde{Q}_\mu(x_0, a)$ as a function of μ, for fixed x_0 and a. In Fig. 3(a) we show the data for $a = 0.5$ and four different values of x_0. For small x_0, the curve has a single minimum at a nonzero value of $\mu^\star_{\text{cap}}(x_0, a)$, while there is a local maximum at $\mu = 0$. As x_0 increases to some value x_m, the derivative of $\widetilde{Q}_\mu(x_0, a)$ with respect to μ at $\mu = 0^+$ [61] vanishes, i.e., $\partial_\mu \widetilde{Q}_\mu(x_m, a)|_{\mu=0} = 0$. This value of x_m can be determined analytically [see Eq. (7) below] and is given by $x_m = e^{-\gamma_E} = 0.561459\ldots$, where γ_E is the Euler constant. When x_0 slightly exceeds x_m, the curve has two minima: one at $\mu = 0^+$ and one at $\mu = \mu^\star_{\text{cap}}(x_0, a)$, but the value at $\mu = 0^+$ is higher. This situation persists for $x_m < x_0 < x_c(a)$. When x_0 exceeds $x_c(a)$, the local minimum at $\mu = 0^+$ becomes the global one and $\mu^\star_{\text{cap}}(x_0, a)$ drops to 0^+, triggering a first-order transition. The point $x_c(a)$ is thus determined by

$$\partial_\mu \widetilde{Q}_\mu(x_c, a)|_{\mu^\star_{\text{cap}}(x_c)} = 0, \quad \widetilde{Q}_\mu(x_c, a)|_{\mu^\star_{\text{cap}}(x_c)} = q_0, \quad (6)$$

where $q_0 \equiv \widetilde{Q}_{\mu=0}(x_c, a)$. From Eq. (4), $q_0 = 1/\sqrt{(1-a)(1-ae^{-1})}$, independent of the position (see [48]). This scenario presented above for $a = 0.5$ continues to hold up to $a = a_1 \approx 0.926$.

For $a > a_1$, a different scenario occurs as displayed in Fig. 3(b) where, again, $\widetilde{Q}_\mu(x_0, a)$ is plotted as a function of μ for different values of x_0. In contrast to Fig. 3(a), the curves always have a single minimum at $\mu = \mu^\star_{\text{cap}}(x_0, a)$ that decreases continuously to 0^+ as x_0 approaches a critical value $x_c(a) = x_m$, signaling a second-order phase transition. Thus, the first and second-order phase transitions merge at $a = a_1$, making it a tricritical point. These numerical observations lead to the phase diagram presented in Fig. 2.

The CMFPT exhibits the same qualitative features as above, with a tricritical point now located at $a = a_2 \approx 0.974\ldots$. In Fig. 3(c), we plot $\mu^\star_{FP}(x_0, a)$ as a function of x_0 for four different values of a close to a_2. The jump discontinuity at $x_0 = x_c(a)$ is finite for $a < a_2$ while it vanishes for $a \geqslant a_2$, confirming indeed that $(x_0 = x_m, a = a_2)$ is a tricritical point for $\mu^\star_{FP}(x_0, a)$ in the (x_0, a) plane.

We show how a_1 and a_2 can be computed analytically using a standard Landau-like expansion well known in critical phenomena. There, by expanding the free energy in powers of the order parameter, the Landau theory gives access to the phase diagram close to a continuous critical/tricritical point. Here we follow the same spirit with μ playing the role of the "order parameter." We then expand $\widetilde{Q}_\mu$ in powers of μ near $\mu = 0^+$: $\widetilde{Q}_\mu(x_0, a) = q_0 + q_1\mu + q_2\mu^2/2! + q_3\mu^3/3! + q_4\mu^4/4! + \ldots$, where the dependence of the q_i's on x_0 and a is implicit. Depending on these parameters, the signs of q_i's in this expansion may change, leading either to a first or second order transition and also to the possibility of a tricritical point. In the standard Landau's theory with a positive order parameter, it is enough to keep terms up to order $O(\mu^3)$ and a tricritical point occurs when $q_1 = q_2 = 0$ while $q_3 > 0$ [62] (see also [63] in the context of stochastic resetting). However, in our case, the dependence of q_i's on x_0 and a are such that this standard scenario is not realized and one needs to keep terms up to order $O(\mu^4)$. From Eq. (4), we show that [48]

$$q_1 = \frac{ae^{-1}}{2\sqrt{1-a}(1-ae^{-1})^{3/2}}(\ln x_0 + \gamma_E), \quad (7)$$

$$q_2 = \frac{3\sqrt{e}a^2}{4\sqrt{1-a}(e-a)^{5/2}}(\ln x_0 + \gamma_E)^2. \quad (8)$$

For $x_0 < x_m = e^{-\gamma_E}$, we have $q_1 < 0$ and $q_2 > 0$. In contrast, for $x_0 > x_m$, we have both $q_1, q_2 > 0$ and both of them vanish simultaneously at $x_0 = x_m$, for any a. The tricritical point thus occurs when $q_3(x_m, a)$ changes sign. We have [48]

$$q_3(x_m, a) = \frac{a\sqrt{e}K}{8\sqrt{1-a}(e-a)^{7/2}}(11a^2 + 8ea - 4e^2), \quad (9)$$

where $K = 2\zeta(3) = 2.40411\ldots$. Thus, $q_3(x_m, a) < 0$ for $a < a_1$ where $a_1 = 2e(\sqrt{15} - 2)/11$ is the unique root of $11a^2 + 8ea - 4e^2 = 0$ in (0,1). At the transition point $x_0 = x_c(a)$ and for $a < a_1$, since $q_3 < 0$, we need to keep terms up to order $O(\mu^4)$ (assuming that $q_4 > 0$ in the Landau expansion). From Eq. (6), the first-order jump discontinuity $\Delta(a) \equiv \mu^\star_{\rm cap}(x_c(a), a)$ is given by [48]

$$\Delta(a) = \frac{2}{3\,q_4}(2|q_3| + \sqrt{4q_3^2 - 9q_2q_4})|_{x_0=x_c(a)}. \quad (10)$$

This discontinuity vanishes when $q_3 \to 0$ and $q_2 \to 0$, which occurs at the point $(x_0 = x_m, a = a_1)$, indicating that this is a tricritical point. If $a > a_1$, then $q_2 > 0$ and $q_3 > 0$; when q_1 changes sign (always at $x_0 = x_m$), a second-order transition occurs. Hence, $x_c(a)$ freezes to x_m for $a > a_1$. A similar Landau-like expansion can be carried out exactly for the CMFPT, which leads to the same qualitative conclusions, with $a_2 = 0.973989\ldots$ [48].

As mentioned before, for a permanent target ($a = 1$), there is no optimal strategy since the capture probability is one and the CMFPT infinite, irrespective of μ. However, it is very important to notice that, for long-lived targets, there is a nontrivial optimal strategy characterized by the same $\mu^*_{\rm cap} = \mu^*_{FP}$ for both observables.

As $a \to 1$, Eqs. (4) and (3) imply $\widetilde{Q}_\mu(x_0, a) \approx g_\mu(x_0)/\sqrt{1-a}$ and $T_{\mu(x_0,a)} \approx g_\mu(x_0)/(2\sqrt{1-a})$, where $g_\mu(x_0)$ is independent of a. Hence, both the capture probability and the CMFPT are optimized by minimizing $g_\mu(x_0)$ with respect to μ. Since the expression of $g_\mu(x_0)$ is complicated, it is hard to obtain the full functional form of $\mu^*_{\rm cap} = \mu^*_{FP}$ for all x_0. However, close to the transition point x_m, where $\mu^*_{\rm cap}$ is expected to be small due to the continuous transition, g_μ directly follows from the small μ expansion of Q_μ above. Using Eqs. (7) and (9), we obtain exactly the leading order for small $(x_m - x_0)/x_m$

$$\mu^*_{\rm cap} = \mu^\star_{FP} \approx A\left(\frac{x_m - x_0}{x_m}\right)^{1/2}, \; x_0 < x_m, \quad (11)$$

where $A = 2(e-1)/\sqrt{\zeta(3)(11 + 8e - 4e^2)} = 1.7549\ldots$ (see the SM [48] for more details). This shows that the limit $a \to 1$ does allow an optimization with respect to μ.

So far, we have analyzed the exact formula in Eq. (4) in the small μ limit. When $a \to 1$ and $x_0 \to 0$, far from x_m, a small x_0 expansion in [48] gives $\mu^\star_{\rm cap} \to 0.905954\ldots$, as indicated in Fig. 2. But to obtain analytically the full curves in Figs. 3(a) and 3(b), as a function of μ from Eq. (4) for any (x_0, a), is extremely hard. Yet, we have found a concavity approximation allowing a very accurate analytical estimate of $\widetilde{Q}_\mu(x_0, a)$. Starting from the concavity of the logarithm, we approximate $\sum_i w_i \ln(r_i) \approx \ln(\sum_i w_i r_i)$ for any set of positive real r_i and normalized weights $\sum_i w_i = 1$. With this, one can perform the inverse Laplace transform in Eq. (4) and deduce the general expression

$$\widetilde{Q}_{\mu,\rm approx}(x_0, s) = \frac{1}{\sqrt{1-s}}e^{-\frac{1}{\pi}\int_0^\infty \ln[1-s\hat{f}(k)]\frac{\sin(kx_0)}{k}dk}, \quad (12)$$

where we have used the identity $\mathcal{L}^{-1}[k/(\lambda^2 + k^2)] = \sin(kx_0)$ for $x_0 > 0$ (see also [48]). Equation (12) is easy to evaluate numerically. Interestingly, the first two terms of its small μ expansion coincide with the exact expressions q_0 and q_1 above, as well as the first terms of its small x_0 expansion [48]. Consequently, Eq. (12) gives the correct slope-change point x_m and captures qualitatively the order of the transitions [see the dashed lines in Figs. 3(a) and 3(b)], along with the existence of a tricritical point. Equation (12) also predicts the optimal exponent for long-lived targets, see the dots of Fig. 3(c).

We conclude with the remark that this problem of a finite-lived target is reminiscent of a Lévy flight subject to resetting with a probability r to its initial position. The mean first-passage time (MFPT) to find a permanent target at the origin was computed for the resetting Lévy flight [17] where the walker has two parameters μ and r that can be used to optimize the MFPT (see also [64] for a related problem). Indeed, the optimal pair (μ^*, r^*) was computed and found to undergo a first-order transition at a critical value of the initial distance x_0 from the target. This is rather different from our problem where the Lévy flight has only a single parameter μ, which can vary to optimize the MFPT. In our model, the walker has no control over the parameter a associated with the lifetime of the target. Hence, here we optimize the search strategy by varying only μ for fixed a, which leads to a new phase diagram with a tricritical point.

In summary, we have studied a simple model of a Lévy flight of index μ in one-dimension searching for a finite-lived target at the origin with mean lifetime $1/(1-a)$. We have shown that the capture probability of the target can be maximized by choosing an optimal $\mu^\star_{\rm cap}$ for fixed a and x_0 (where x_0 denotes the initial distance from the target). The presence of a finite lifetime leads to a very rich and nontrivial phase diagram for $\mu^\star_{\rm cap}$ in the (x_0, a) plane. This work opens up many interesting possibilities for future works. For instance, it would be interesting to find the optimal strategy in higher dimensions, for multiple Lévy flights and for the case where the distribution of the target lifetime is nonexponential.

D.B. acknowledges support from the LPTMS at the Université Paris-Saclay (France) and from CONACYT (Mexico) Grant Ciencia de Frontera 2019/10872. We thank Lya Naranjo Pineda for illustration support in Fig. 1.

[1] F. Bartumeus and J. Catalan, Optimal search behavior and classic foraging theory, J. Phys. A: Math. Theor. **42**, 434002 (2009).

[2] G. M. Viswanathan, M. G. da Luz, E. P. Raposo, and H. E. Stanley, *The Physics of Foraging: An Introduction to Random Searches and Biological Encounters* (Cambridge University Press, Cambridge, 2011).

[3] M. Serra, P. Sathe, I. Rypina, A. Kirincich, S. D. Ross, P. Lermusiaux, A. Allen, T. Peacock, and G. Haller, Search and

rescue at sea aided by hidden flow structures, Nat. Commun. **11**, 2525 (2020).

[4] V. Kosmas, M. Acciaro, and M. Besiou, Saving migrants lives at sea: Improving search and rescue operations, Prod. Oper. Manag. **31**, 1872 (2022).

[5] M. F. Shlesinger and J. Klafter, Lévy walks versus Lévy flights, in *On Growth and Form: Fractal and Non-Fractal Patterns in Physics*, edited by H. E. Stanley and N. Ostrowsky (M. Nijhoff, Dordrecht, 1986), pp. 279–283.

[6] G. M. Viswanathan, S. V. Buldyrev, S. Havlin, M. G. E. da Luz, E. P. Raposo, and H. E. Stanley, Optimizing the success of random searches, Nature (London) **401**, 911 (1999).

[7] F. Bartumeus and S. A. Levin, Fractal reorientation clocks: Linking animal behavior to statistical patterns of search, Proc. Natl. Acad. Sci. **105**, 19072 (2008).

[8] N. Levernier, J. Textor, O. Bénichou, and R. Voituriez, Inverse square Lévy walks are not optimal search strategies for $d \geqslant 2$, Phys. Rev. Lett. **124**, 080601 (2020).

[9] S. V. Buldyrev, E. P. Raposo, F. Bartumeus, S. Havlin, F. R. Rusch, M. G. E. da Luz, and G. M. Viswanathan, Comment on Inverse square Lévy walks are not optimal search strategies for $d \geqslant 2$, Phys. Rev. Lett. **126**, 048901 (2021).

[10] N. Levernier, J. Textor, O. Bénichou, and R. Voituriez, Reply to Comment on Inverse square Lévy walks are not optimal search strategies for $d \geqslant 2$, Phys. Rev. Lett. **126**, 048902 (2021).

[11] B. Guinard and A. Korman, Intermittent inverse-square Lévy walks are optimal for finding targets of all sizes, Sci. Adv. **7**, eabe8211 (2021).

[12] A. Clementi, F. d'Amore, G. Giakkoupis, and E. Natale, Search via parallel Lévy walks on $\mathbb{Z}^2$, in *Proceedings of the 2021 ACM Symposium on Principles of Distributed Computing* (ACM, New York, 2021), pp. 81–91.

[13] G. Oshanin, H. Wio, K. Lindenberg, and S. Burlatsky, Intermittent random walks for an optimal search strategy: one-dimensional case, J. Phys.: Condens. Matter **19**, 065142 (2007).

[14] O. Bénichou, C. Loverdo, M. Moreau, and R. Voituriez, Intermittent search strategies, Rev. Mod. Phys. **83**, 81 (2011).

[15] M. R. Evans and S. N. Majumdar, Diffusion with stochastic resetting, Phys. Rev. Lett. **106**, 160601 (2011).

[16] M. R. Evans and S. N. Majumdar, Diffusion with optimal resetting, J. Phys. A: Math. Theor. **44**, 435001 (2011).

[17] L. Kusmierz, S. N. Majumdar, S. Sabhapandit, and G. Schehr, First order transition for the optimal search time of Lévy flights with resetting, Phys. Rev. Lett. **113**, 220602 (2014).

[18] S. Reuveni, M. Urbakh, and J. Klafter, Role of substrate unbinding in Michaelis–Menten enzymatic reactions, Proc. Natl. Acad. Sci. **111**, 4391 (2014).

[19] E. Roldán, A. Lisica, D. Sánchez-Taltavull, and S. W. Grill, Stochastic resetting in backtrack recovery by RNA polymerases, Phys. Rev. E **93**, 062411 (2016).

[20] A. Pal and S. Reuveni, First passage under restart, Phys. Rev. Lett. **118**, 030603 (2017).

[21] A. Falcón-Cortés, D. Boyer, L. Giuggioli, and S. N. Majumdar, Localization transition induced by learning in random searches, Phys. Rev. Lett. **119**, 140603 (2017).

[22] M. R. Evans, S. N. Majumdar, and G. Schehr, Stochastic resetting and applications, J. Phys. A: Math. Theor. **53**, 193001 (2020).

[23] A. Pal, S. Kostinski, and S. Reuveni, The inspection paradox in stochastic resetting, J. Phys. A: Math. Theor. **55**, 021001 (2022).

[24] M. R. Evans and S. N. Majumdar, Diffusion with resetting in arbitrary spatial dimension, J. Phys. A: Math. Theor. **47**, 285001 (2014).

[25] A. Pal, A. Kundu, and M. R. Evans, Diffusion under time-dependent resetting, J. Phys. A: Math. Theor. **49**, 225001 (2016).

[26] S. Reuveni, Optimal stochastic restart renders fluctuations in first passage times universal, Phys. Rev. Lett. **116**, 170601 (2016).

[27] M. Montero and J. Villarroel, Directed random walk with random restarts: The Sisyphus random walk, Phys. Rev. E **94**, 032132 (2016).

[28] U. Bhat, C. De Bacco, and S. Redner, Stochastic search with Poisson and deterministic resetting, J. Stat. Mech.: Theory Exp. (2016) 083401.

[29] G. Mercado-Vásquez, D. Boyer, S. N. Majumdar, and G. Schehr, Intermittent resetting potentials, J. Stat. Mech.: Theory Exp. (2020) 113203.

[30] P. C. Bressloff, Diffusive search for a stochastically-gated target with resetting, J. Phys. A: Math. Theor. **53**, 425001 (2020).

[31] B. De Bruyne, S. N. Majumdar, and G. Schehr, Optimal resetting Brownian bridges via enhanced fluctuations, Phys. Rev. Lett. **128**, 200603 (2022).

[32] G. Mercado-Vásquez, D. Boyer, and S. N. Majumdar, Reducing mean first passage times with intermittent confining potentials: a realization of resetting processes, J. Stat. Mech.: Theory Exp. (2022) 093202.

[33] M. Biroli, S. N. Majumdar, and G. Schehr, Critical number of walkers for diffusive search processes with resetting, Phys. Rev. E **107**, 064141 (2023).

[34] O. Tal-Friedman, A. Pal, A. Sekhon, S. Reuveni, and Y. Roichman, Experimental realization of diffusion with stochastic resetting, J. Phys. Chem. Lett. **11**, 7350 (2020).

[35] B. Besga, A. Bovon, A. Petrosyan, S. N. Majumdar, and S. Ciliberto, Optimal mean first-passage time for a Brownian searcher subjected to resetting: experimental and theoretical results, Phys. Rev. Res. **2**, 032029(R) (2020).

[36] F. Faisant, B. Besga, A. Petrosyan, S. Ciliberto, and S. N. Majumdar, Optimal mean first-passage time of a Brownian searcher with resetting in one and two dimensions: experiments, theory and numerical tests, J. Stat. Mech.: Theory Exp. (2021) 113203.

[37] K. R. Janmaat, R. W. Byrne, and K. Zuberbühler, Primates take weather into account when searching for fruits, Curr. Biol. **16**, 1232 (2006).

[38] P. Tikuisis, Prediction of survival time at sea based on observed body cooling rates, Aviat. Space Environ. Med. **68**, 441 (1997).

[39] I. Golding, J. Paulsson, S. M. Zawilski, and E. C. Cox, Real-time kinetics of gene activity in individual bacteria, Cell **123**, 1025 (2005).

[40] O. K. Wong, M. Guthold, D. A. Erie, and J. Gelles, Interconvertible lac repressor–DNA loops revealed by single-molecule experiments, PLoS Biol. **6**, e232 (2008).

[41] Y.-J. Chen, S. Johnson, P. Mulligan, A. J. Spakowitz, and R. Phillips, Modulation of DNA loop lifetimes by the free energy of loop formation, Proc. Natl. Acad. Sci. **111**, 17396 (2014).

[42] S. Waharte and N. Trigoni, Supporting search and rescue operations with UAVs, in *2010 International Conference on Emerging Security Technologies* (IEEE, 2010) pp. 142–147.
[43] E. L. Charnov, Optimal foraging, the marginal value theorem, Theoretical Population Biology **9**, 129 (1976).
[44] S. B. Yuste, E. Abad, and K. Lindenberg, Exploration and trapping of mortal random walkers, Phys. Rev. Lett. **110**, 220603 (2013).
[45] B. Meerson and S. Redner, Mortality, redundancy, and diversity in stochastic search, Phys. Rev. Lett. **114**, 198101 (2015).
[46] S. Belan, Restart could optimize the probability of success in a Bernoulli trial, Phys. Rev. Lett. **120**, 080601 (2018).
[47] M. Radice, Effects of mortality on stochastic search processes with resetting, Phys. Rev. E **107**, 024136 (2023).
[48] See Supplemental Material at http://link.aps.org/supplemental/10.1103/PhysRevE.109.L022103 for details of the calculations, which also includes Refs. [17,49–51].
[49] E. Sparre Andersen, On the fluctuations of sums of random variables II, Mathematica Scandinavica **2**, 195 (1954).
[50] H. Stehfest, Algorithm 368: Numerical inversion of Laplace transforms [d5], Commun. ACM **13**, 47 (1970).
[51] K. L. Kuhlman, Review of inverse Laplace transform algorithms for Laplace-space numerical approaches, Numerical Algorithms **63**, 339 (2013).
[52] F. Pollaczek, Fonctions caractéristiques de certaines répartitions définies au moyen de la notion d'ordre. Application à la théorie des attentes, C. R. Acad. Sci. Paris **234**, 2334 (1952).
[53] F. Spitzer, A combinatorial lemma and its application to probability theory, Trans. Amer. Math. Soc. **82**, 323 (1956).
[54] S. Redner, *A Guide to First-Passage Processes* (Cambridge University Press, Cambridge, 2001).
[55] A. Comtet and S. N. Majumdar, Precise asymptotics for a random walkers maximum, J. Stat. Mech.: Theory Exp. (2005) P06013.
[56] S. N. Majumdar, Universal first-passage properties of discrete-time random walks and Lévy flights on a line: Statistics of the global maximum and records, Physica A **389**, 4299 (2010).
[57] A. J. Bray, S. N. Majumdar, and G. Schehr, Persistence and first-passage properties in nonequilibrium systems, Adv. Phys. **62**, 225 (2013).
[58] S. N. Majumdar, P. Mounaix, and G. Schehr, Survival probability of random walks and Lévy flights on a semi-infinite line, J. Phys. A: Math. Theor. **50**, 465002 (2017).
[59] J. Klinger, R. Voituriez, and O. Bénichou, Splitting probabilities of symmetric jump processes, Phys. Rev. Lett. **129**, 140603 (2022).
[60] W. Feller, *An Introduction to Probability Theory and Its Applications* (John Wiley & Sons, 2008), Vol 1.
[61] Here we consider the $\mu \to 0^+$ limit (and not strictly $\mu = 0$). In the limit $\mu \to 0^+$ the jump distribution is normalizable but not when $\mu = 0$ exactly. Hence we restrict only to the case $\mu \to 0^+$.
[62] J. M. Kincaid and E. G. D. Cohen, Phase diagrams of liquid helium mixtures and metamagnets: experiment and mean field theory, Phys. Rep. **22**, 57 (1975).
[63] A. Pal and V. V. Prasad, Landau-like expansion for phase transitions in stochastic resetting, Phys. Rev. Res. **1**, 032001(R) (2019).
[64] D. Campos and V. Méndez, Phase transitions in optimal search times: How random walkers should combine resetting and flight scales, Phys. Rev. E **92**, 062115 (2015).